applied sciences

MDPI

Article

Creating a Novel Mathematical Model of the Kv10.1 Ion Channel and Controlling Channel Activity with Nanoelectromechanical Systems

Jasmina Lozanović Šajić [1,2,*], Sonja Langthaler [1] and Christian Baumgartner [1]

[1] Institute of Health Care Engineering with European Testing Center for Medical Devices, Graz University of Technology, A-8010 Graz, Austria; s.langthaler@tugraz.at (S.L.); christian.baumgartner@tugraz.at (C.B.)
[2] Innovation Center of the Faculty of Mechanical Engineering, University of Belgrade, 11000 Belgrade, Serbia
* Correspondence: j.lozanovicsajic@tugraz.at

Featured Application: Nanoelectromechanical systems and nanorobots can be used to treat cancers associated with the Kv10.1 voltage-gated ion channel activity. The Kv10.1 model was developed by applying the control engineering theory. Nanoelectromechanical systems play the role of a PID regulator.

Abstract: The use of nanoelectromechanical systems or nanorobots offers a new concept for sensing and controlling subcellular structures, such as ion channels. We present here a novel method for mathematical modeling of ion channels based on control system theory and system identification. We investigated the use of nanoelectromechanical devices to control the activity of ion channels, particularly the activity of the voltage-gated ion channel Kv10.1, an important channel in cancer development and progression. A mathematical model of the dynamic behavior of the selected ion channel Kv10.1 in the Laplace (s) domain was developed, which is given in the representation of a transfer function. In addition, we addressed the possibilities of controlling ion channel activity by nanoelectromechanical devices and nanorobots and finally presented a control algorithm for the Kv10.1 as a control object. A use case demonstrates the potential of a Kv10.1 controlled nanorobot for cancer treatment at a single-cell level.

Keywords: nanoelectromechanical system (NEMS); nanorobots; ion channel Kv10.1; mathematical modeling; system identification; control algorithm

Citation: Šajić, J.L.; Langthaler, S.; Baumgartner, C. Creating a Novel Mathematical Model of the Kv10.1 Ion Channel and Controlling Channel Activity with Nanoelectromechanical Systems. *Appl. Sci.* **2022**, *12*, 3836. https://doi.org/10.3390/app12083836

Academic Editors: Luis Gracia and Carlos Perez-Vidal

Received: 14 March 2022
Accepted: 8 April 2022
Published: 11 April 2022

1. Introduction

Nanoelectromechanical systems, nanomachines, and nanorobots represent a challenging and future-orientated research area in biomedical engineering. A nanoelectromechanical system (NEMS) is a device that combines electrical and mechanical system behavior at the nanoscale level. The NEMS has electromechanical parts that have been developed on the nanoscale level, such as sensors, actuators, controllers, and drives [1]. Nanorobots are nanoelectromechanical or nanomechatronic systems, which are innovative devices expected to have revolutionary applications in health care, cancer therapy, monitoring, and drug delivery [2]. These nanoelectromechanical systems and nanorobots represent miniaturizations of microelectromechanical systems and microrobots that travel in the human body and can be used in applications to monitor, interact, and control processes at a cellular level. In particular, these robotic applications involve sensing, control, actuation and propulsion, communications, interfacing, programming and coordination at macro, micro, and nano-levels [2].

In the field of biomedical engineering and medicine, microelectromechanical/nanoelectromechanical systems (MEMS/NEMS) are also called bioMEMS/bioNEMS [3],

with almost unlimited practical applications, e.g., in surgery, drug delivery, or gene therapy [4–8]. Figure 1 shows a schematic nanoscale comparison of different items in nature, adapted based on material published in [3,9].

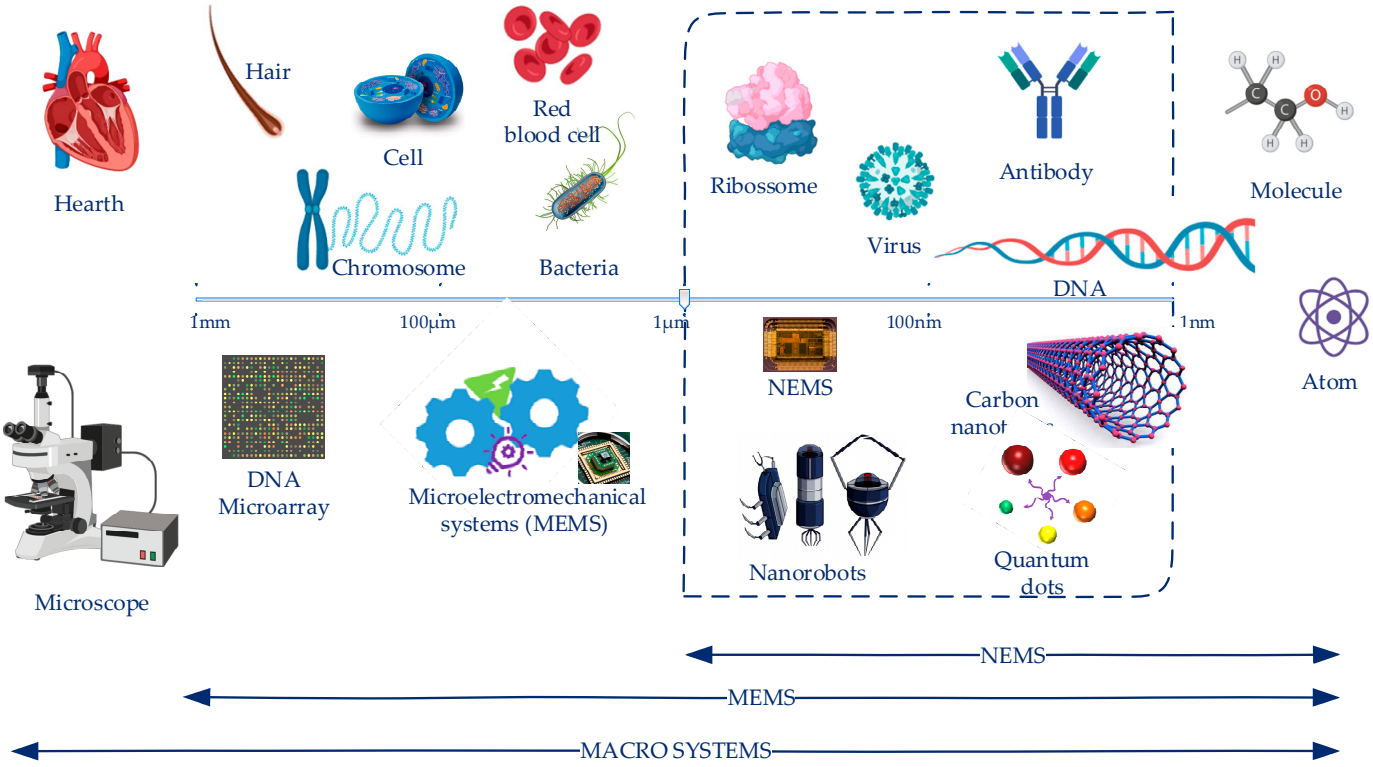

Figure 1. Scales in nature, ranging from micro-systems to nano-systems.

In this work, we chose a voltage-gated potassium ion channel as an example of a biological system at a nanoscale. Ion channels are membrane proteins the size of about 4 nm that enable the passive transport of ions through the cell membrane [10,11]. Based on the scale depicted in Figure 1, we assumed that the dynamic behavior of the ion channel could be measured and controlled with MEMS/NEMS and/or nanorobots. Depending on the gating mechanism, three main types of ion channels are classified as: voltage-gated, receptor/ligand-gated, and second messenger gated channels [12]. Cells usually express a variety of ion channel types, e.g., there are more than 300 different ion channels in an inner ear cell alone [13].

We here selected a single channel from a voltage-gated ion channel family representing the biological system. Voltage-gated ion channels open (activate) and close depending on the cell membrane potential. Subtypes of voltage-gated ion channels (Nav, Cav, Kv, CLC, and Hv) are specifically selective for sodium (Na^+), calcium (Ca^{2+}), potassium (K^+), chloride (Cl^-), and proton (H^+) channels. Voltage-gated potassium channels are referred to as the giant subtype and denoted as Kv. These Kv channels encode more than 100 human genes [14]. Potassium channels represent the most complex class of voltage-gated channels [15] and are found in basically all types of mammalian cells, such as cells in the nervous, muscular, and immune systems, among others [15–18].

Each ion channel exhibits a specific dynamic behavior with different physiological and pharmacological properties [15]. In particular, aberrant expression and functionality of various Kv channels in cancer cells have been associated with tumor development and progression. The voltage-gated Kv10.1 potassium channel, encoded by the gene KCNH1 (subfamily H member 1, known as EAG1 or Ether-à-go-go 1), is implicated in various cellular processes, including, for example, cell proliferation [15].

An analysis of Kv channel expression in human cancer cells [18] revealed an up-regulation of Kv10.1 in a variety of tumors and can be found in blood, bone, brain, breast, stomach, colon, cervix cancer, and prostate cancers cells, thus providing a novel biomarker candidate and potential oncological target for cancer [5,19,20].

For single-channel modeling, we finally selected the Kv10.1 ion channel, as it represents a significant ion channel in cancer development and progression. The Kv10.1 model is based on control system theory, which is similarly based on the modeling concept of the Kv1.1 voltage-gated channel recently presented in [21].

2. Methods

For mathematical modeling of voltage-gated ion channels, the method of system identification known from control engineering was used. We considered the voltage-gated ion channel Kv10.1 as a system, object, or process in accordance with the control system theory. Kv10.1 was treated as a separate object (or system/process) within a space that can interact or connect with other elements. If a system is interpreted as a combination of elements that act together and perform specific objectives [22], then a single ion channel can be considered as a system or, in more precise terms, as an object in a control loop. As such, the channel can achieve the desired dynamics under nominal conditions and display acceptable behaviors under random conditions that deviate from the maximum prescribed boundary conditions.

System identification is a scientific methodology that is used to develop mathematical models of a dynamical system. This method is based on observed or measured data of the system [23]. A block diagram of a general system ($G(s)$) represents a transfer function with a complex variable s in the Laplace domain, specified with an input $c(t)$, output $r(t)$, measured disturbances $dc(t)$, and unmeasured disturbances $d(t)$ (Figure 2a). An illustration of a voltage-gated ion channel as a system is shown in Figure 2b. The block diagram of the system shows its unilateral property, where system inputs and outputs, in general, are vectors. If there are multiple inputs and multiple outputs, then the system is called a MIMO system. In the case of a single input and a single output, however, the control system is called a SISO system. For example, if a voltage-gated ion channel has a voltage stimulus as input and a measured current as output, we assume that it can be described as a SISO system.

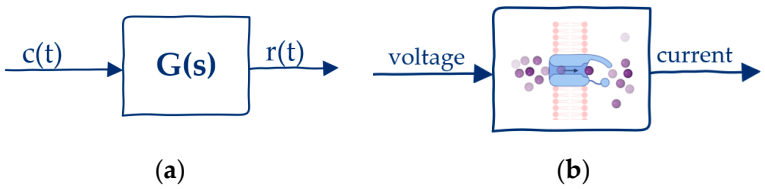

Figure 2. Block diagram of a system (**a**); illustrated voltage-gated ion channel as a system (**b**).

Furthermore, we assume that the voltage-gated ion channel Kv10.1 is a linear time-invariant system based on the experimental results given in the following sections. A linear time-invariant system is defined by

$$\begin{aligned} &a_n r^{(n)}(t) + a_{n-1} r^{(n-1)}(t) + \ldots + a_1 \dot{r}(t) + a_0 r(t) = \\ &b_0 c(t) + b_1 \dot{c}(t) + \ldots + b_{n-1} c^{(n-1)}(t) + b_n c^{(n)}(t), \quad n \geq m. \end{aligned} \tag{1}$$

where $r(t)$ is the system's output and $c(t)$ is the system's input. The transfer function, $G(s)$, is defined as the ratio of the left Laplace-transformed output and the left Laplace-transformed input under zero initial conditions, where s is a complex variable in the Laplace (S) domain.

$$G(s) = \frac{\mathcal{L}\{r(t)\}}{\mathcal{L}\{c(t)\}} = \frac{R(s)}{C(s)} = \frac{b_0+b_1s+...+b_{n-1}s^{n-1}+b_ns^n}{a_ns^n+a_{n-1}s^{n-1}+...+a_1\dot{y}(t)+a_0y(t)} = \\ = \frac{\sum_0^m b_ms^m}{\sum_0^n a_ns^n} \quad (2)$$

The application of the transfer function concept makes it possible to represent the system's dynamics in the form of algebraic equations. If the highest power of s in the denominator of a transfer function is equal to n, the system is called an nth-order system [22]. The transfer function of a system is thus a mathematical model of this system. If the system's transfer function is unknown, we can estimate it based on known inputs and measured outputs for the system. This resulting transfer function provides a complete description of the system's dynamic behavior [22,24,25].

A transfer function can be determined experimentally based on measured input and output signals if a mathematical model cannot be developed using physical correlations and equations. Therefore, the process of developing a model from measured input and output data is known as system identification [23,26]. The main elements in the system identification process cycle are experimental design, the experiment itself, data preprocessing, fitting the model to the data, testing the model structure, validating and auditing the model [26].

The process of system identification has been greatly simplified due to the availability of modern software tools, such as MATLAB or LabVIEW. In this work, we used the System Identification toolbox provided by MATLAB [27,28]. This toolbox includes tools to identify a modeling approach and to define the model structure properties. Measured data can be imported as time-domain or frequency-domain data, and functions for preprocessing, representing, filtering, and estimating the model can be applied. Furthermore, a model can be estimated as a transfer function, a state-space, process, polynomial, or nonlinear model by the System Identification toolbox.

3. Results

We considered experimental patch-clamp data [15] from CHO (Chinese hamster ovary) host cells, stably expressing rat Kv10.1 channels, which exhibit a highly comparable electrophysiological behavior to human Kv10.1 channels [29]. The data provided comprises voltage-clamp measurements at three different temperature levels of 15, 25, and 35 °C. The dynamic behavior of the voltage-gated ion channels displays three main characteristics: activation, deactivation, and inactivation (Figure 3). In the case of the depolarization of the cell membrane, the Kv channel transits from the resting (closed) to the active (open) state. During prolonged depolarization, Kv channels switch to an inactivated state [30]. Figure 3 shows the whole-cell current response to applied voltage-step protocols for the determination of the activation, deactivation, and inactivation characteristics of the channel. In developing the dynamic behavior of the system, the three different stimulus signals, as shown in Figure 3, were used to provoke these activities. In addition, these activation, deactivation, and inactivation characteristics could also be stimulated alternatively by ramp, action potential (AP), and recovery protocols [15].

For model development, the dynamic behavior of Kv10.1 was considered at a temperature of 25 °C, which corresponds to standard experimental conditions in in vitro electrophysiological studies. The activation or opening is stimulated with appropriate depolarizing input voltage step functions. Nevertheless, the Kv10.1 response corresponds to the transient response of the system. Based on the experimentally measured response to given stimuli, we concluded that Kv10.1 behaves as a first-order system. We assumed all initial conditions as equal to zero and at a nominal voltage of 70 mV. It was possible to obtain an average model based on averaged data for all cells, as given in [21] for the Kv1.1 voltage-gated ion channel. We also considered a randomly chosen active cell with high-quality recording data from the database available via Channelpedia, a web-based freely accessible information management network and electrophysiology data repository [15].

The chosen cell ID is 9514 at 25 °C, and the host cell is CHO_FT; the species is rat. Input and output experimental data from patch-clamp measurements are given in Figure 3.

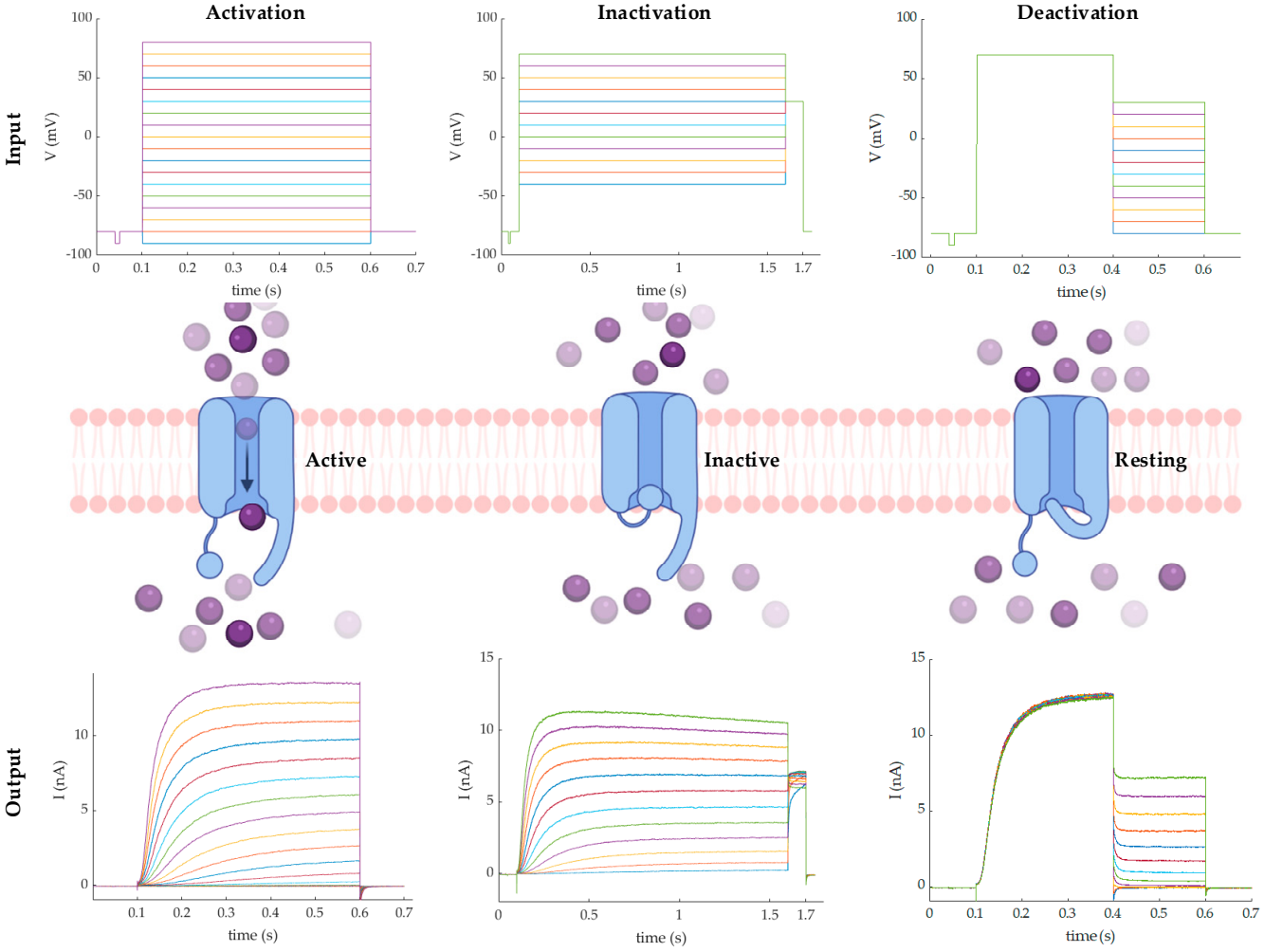

Figure 3. Dynamic behavior of the voltage-gated ion channel Kv10.1. Created with BioRender.

Figure 4 shows the activation voltage step protocol to determine the opening or activation of the ion channel and the measured macroscopic ion current as input and output for system identification. We assumed a nominal operating point at an input voltage of 70 mV, based on the experimental design and input functions for inactivation and deactivation. Input-output data from the patch-clamp experiments for the nominal operating point are shown in Figure 5a. Time-domain experimental data were imported into the System Identification toolbox in MATLAB. The data were not preprocessed and, based on the measured output signal and input step signals, we adopted a first-order linear time-invariant system. A comparison between measured and simulated model output is shown in Figure 5b.

The transfer function was estimated with one pole and null zeros in the continuous-time domain, the i/o delay was fixed to zero, and we set the initial condition to zero. The initialization method implies that the algorithm is used to initialize the numerator and denominator. Algorithms applicable only for estimating continuous-time transfer functions using time-domain data are the instrument variable (IV), state variable filters (SVF), generalized Poisson moment functions (GPMF), subspace state-space estimation (N4SID), and a combination of all of the preceding (ALL) approaches [27,28]. We chose to use the initialization method ALL. This method of systems modeling is known as black-box modeling.

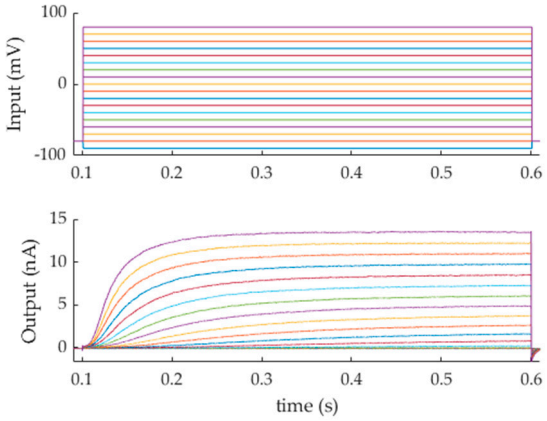

Figure 4. Input: activation voltage step protocol (**above**); output: measured macroscopic ion-current (**below**) for system identification.

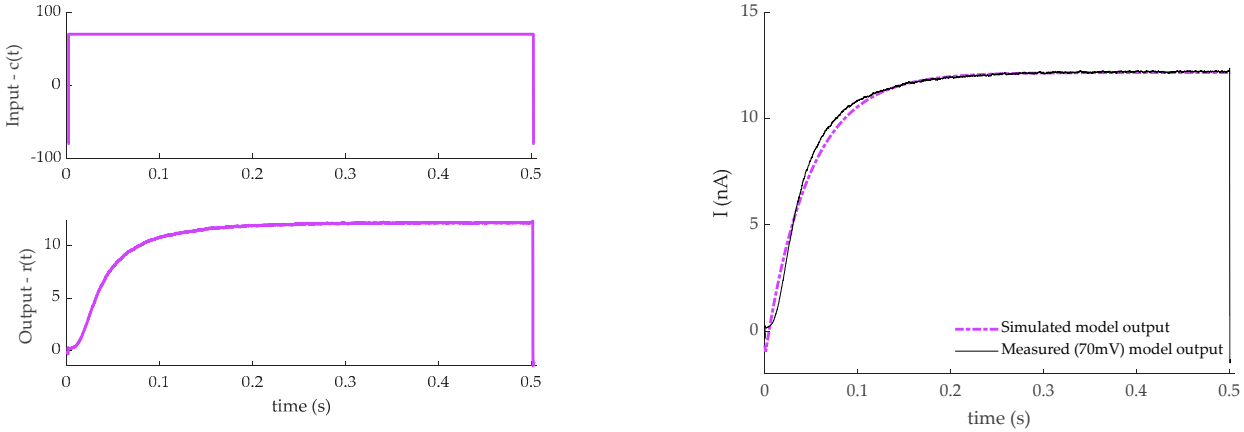

(**a**) (**b**)

Figure 5. Input-output data for nominal operating point at 70 mV (**a**); output: macroscopic ion current (**b**) used for system identification.

The estimated transfer function model for the assumed nominal step input of 70 mV and measured output macroscopic current in nA is given by

$$G(s) = \frac{3.687}{s + 21.22} \tag{3}$$

where units of the transfer function $G(s)$ are ratio units of output (s)—the output macroscopic current (nA), and units of input (s)—the input voltage step (mV).

The model, Equation (3), is written in a general form of a first-order system in the Laplace domain by

$$G(s) = \frac{K}{Ts + 1} \tag{4}$$

where K is the gain with K = 0.1738 and T the time constant, T = 0.0471. The system's gain is the ratio between the input signal and the steady-state value of the output.

4. Discussion

4.1. System Analysis

The mathematical model of the system is given by Equations (3) and (4) in the Laplace domain. The unit step response of the system is shown in Figure 6. Besides the gain and time constant, other essential characteristics of the system are the rise time, transient time, settling time, and steady-state. These system characteristics are calculated from the transfer function or are found by plotting the step response in MATLAB.

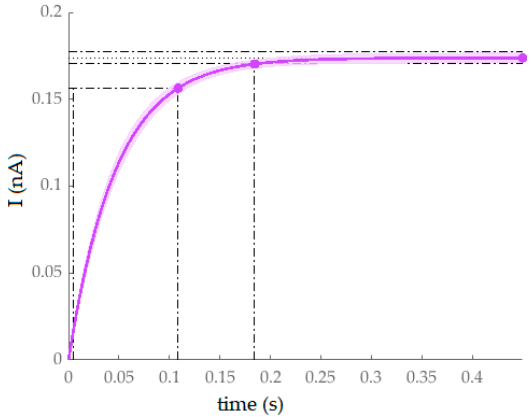

Figure 6. Unit step response of the system $G(s)$ with confidence region.

In Figure 6, the rise time is 0.104 s, the transient time is 0.184 s, and the final value corresponds to a gain of 0.174 nA; thus, the system does not have an overshoot. Experimental output data and the mathematical model indicate that stability is enforced. The same conclusion was drawn by conducting a pole location analysis. The model has one pole with a negative real part, and the system was determined to be stable [22,24,25].

The model in the Laplace domain corresponds to the differential equation under the assumption that all initial conditions are zero [22]. The inverse Laplace transformation gives a solution of a differential equation in the time domain, and the system described with the solution to Equation (4) in the time domain is

$$g(t) = 0.1738\left(1 - e^{\frac{t}{0.0471}}\right)h(t) \tag{5}$$

where $g(t)$ corresponds to $G(s)$, representing the unit step response of the system $G(s)$ (see Figure 6) when all initial conditions are equal to zero, and $h(t)$ is the input function, which corresponds to the unit step or Heaviside function $h(t)$.

We simulated outputs of the model using Equation (4) with inactivation and deactivation stimuli. The compared results of the measured outputs and simulated outputs are shown in Figure 7. The model satisfies the dynamic behavior of the Kv10.1 voltage-gated ion channel based on the adopted assumptions.

Since different cellular mechanisms can affect the opening behavior of ion channels, we believe that time-dependent transfer functions can be used to provide a more accurate description of the dynamic characteristics of ion channels. This hypothesis is supported by the fact that all mathematical systems are non-stationary and that the mathematical origin of non-stationarity can be proved [31].

4.2. Control Algorithm

The model (Equation (3)) is stable, observable, and controllable because the rank of the controllability and observability matrix is equal to n, where $n = 1$, and the system is a first-order system [22,24,25]. We considered a classical control algorithm for the Kv10.1 model. The controller is designed using the Sisotool in MATLAB. We chose an automated tuning method for a PID compensator in a feedback loop, the tuning method is a robust time response, and the controller type is PID. The controller is given by

$$C(s) = 316.85\left(\frac{1 + 0.0026s}{s}\right) \tag{6}$$

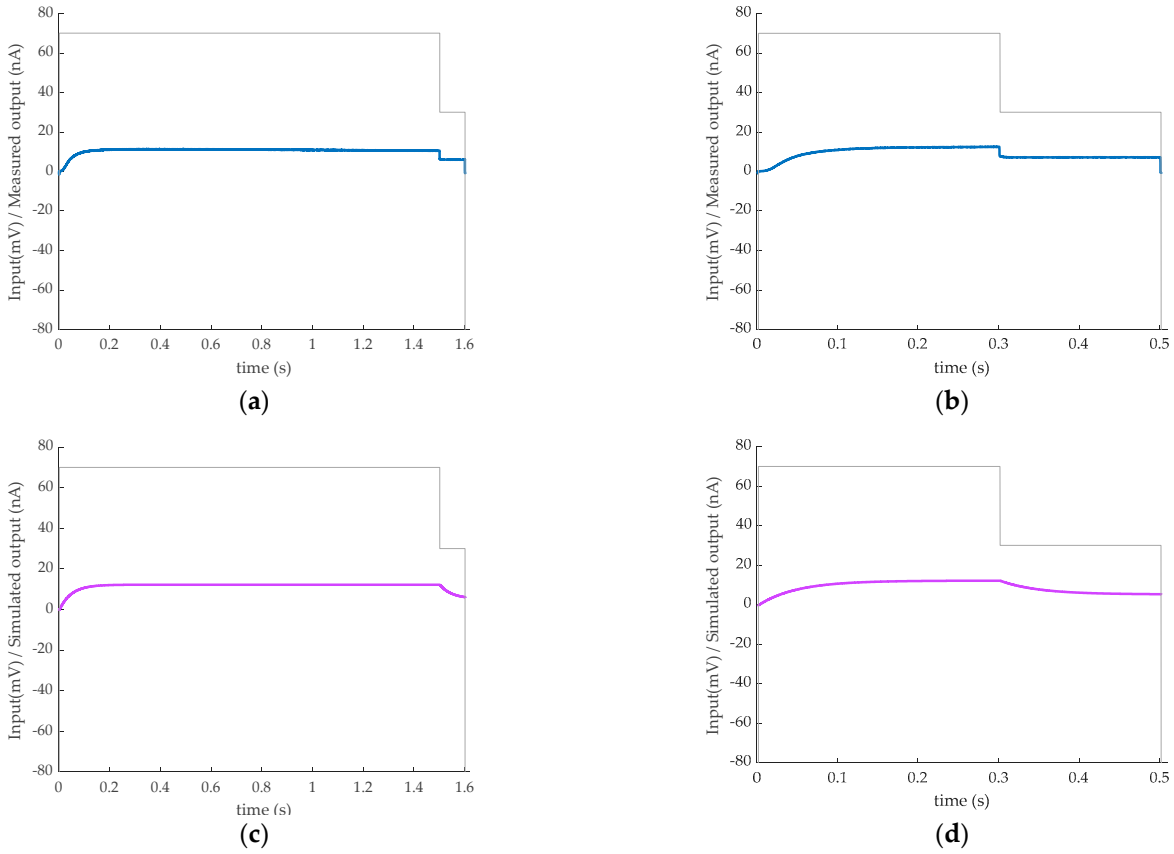

Figure 7. Measured and simulated output macroscopic current for the inactivation and deactivation input stimuli (grey lines). Input stimulus inactivation: measured output (**a**), simulated output (**b**); input stimulus deactivation: measured output (**c**), simulated output (**d**).

The unit step response of the controlled Kv10.1 voltage-gated ion channel in a closed-loop, also called a feedback loop, is shown in Figure 8. The Kv10.1 in the feedback loop displays a rise time of 0.043 s, a peak amplitude of 1.06 nA, an overshoot of 6.08%, a transient time of 0.149 s, and a final value of 1 nA. The controlled model has a faster rise time and transient response, and the final value corresponds to the desired value.

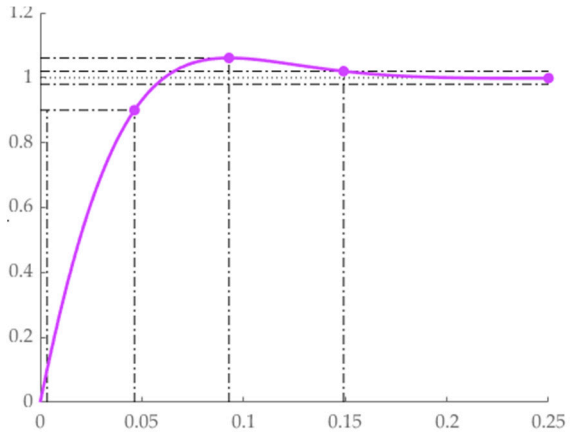

Figure 8. Unit step response of the Kv10.1 model in a control loop.

The feedback control system with the Kv10.1 model, $G(s)$, and controller $C(s)$ in a loop was implemented in Simulink (Figure 9a). A sine waveform with unit amplitude and frequency of 1 Hz was chosen as a simulation input. The simulated output is shown in

Figure 9b. Nevertheless, using this approach of ion channel modeling, the ion channel could be simulated as a single system or a system in a control loop with any randomly chosen input, enabling the obtained output to be analyzed.

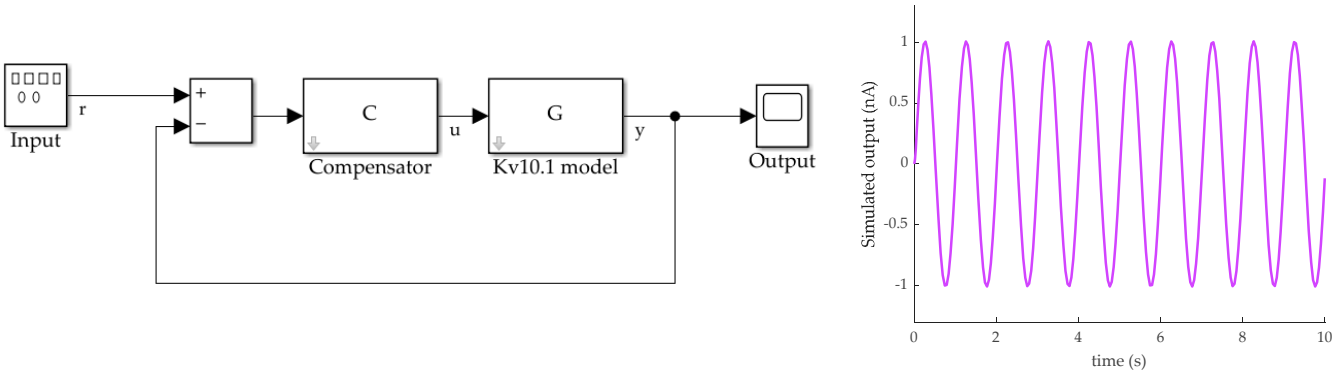

(**a**) (**b**)

Figure 9. Simulink Kv10.1 model in a control loop (**a**); simulated output for sine input (**b**).

Microelectromechanical (MEMS) devices and nanoelectromechanical (NEMS) devices can be designed as MEMS PID controllers and NEMS PID controllers. In a clinical context, nanorobots are already used for the mechanical opening of a cell membrane [32], microscopic surgical procedures, drug delivery, gene therapy, or selective destruction of cancer cells [4]. Therefore, our vision is that free-floating and guided nanorobots could have promising applications in cancer detection and therapy. Research has shown that the up-regulation of the selected channel Kv10.1 can promote cell proliferation and thus tumor development in different organs and human body systems [18], whereas the downregulation of Kv10.1 could potentially have the opposite effect, providing a potential oncological target. However, since the same ion channels are also expressed in normal, healthy cells, albeit to minor expression levels, one of the biggest challenges is to specifically block or manipulate them only in cancer cells. Nanorobots could be programmed to target certain cell clusters, tissues or organs (e.g., prostate, stomach, or breast) and specifically control the activity of selected ion channels in cancer cells without affecting the same channels expressed in surrounding healthy cells or other tissues and thus impairing their function. A controlled down-regulation of the ion channel current in specific cells only would also allow for a systemic application, such as the use of traveling nanorobots for the treatment of cancer in various regions of the body or targeted tissues and cell clusters, as shown in Figure 10, for example.

4.3. Potential Use Case for Treating Breast Cancer Using a Kv10.1 Controlled Nanorobot

Our hypothesis for the use of swimming nanorobots is to control ion-channel activity to specifically target cancer cells in breast tumors. We know that Kv10.1 channels in the nervous system contribute to the control of neuronal excitability. However, since activation requires strong depolarization, a single action potential would not be sufficient for activation [33]. In contrast, cancer cells are usually depolarized so that the channels are predominantly open, providing a potential target for pinpoint destruction by nanorobots. For example, overexpression of Kv10.1 channels is significantly up-regulated in invasive breast carcinoma, whereas healthy breast tissue shows hardly any expression or activity of the Kv10.1 channel [30,33–36]. Floating nanorobots applied via the blood circulation can be guided to the targeted sites and measure and control the Kv10.1 channel activity of the cells in the area of interest. Since nanorobots act as sensors and actuators, if the sensor interface detects an altered behavior of Kv10.1 channel activity, as is the case in breast cancer cells, the channels could be controlled accordingly by the Kv10.1 feedback control system of the robot (see Figures 9 and 10). Alternatively, after detecting a cancer cell based on aberrant or

abnormal channel activity, such MEMS/NEMS-based nanorobot devices may also act as a nano-scalpel that mechanically destroys the targeted cell.

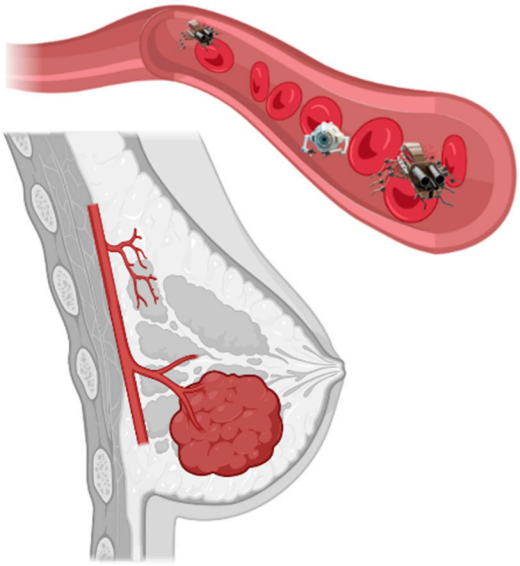

Figure 10. Illustration of possible application of Kv10.1-controlled nanorobots in breast cancer detection and treatment. The cancerous area will be reached by the nanorobots through the blood vessel system. Created with BioRender.

Further examples of possible applications are discussed in [34,37–39]. However, although the practical implementation of this use case has not been performed and validated, this work demonstrates a potential new, forward-looking direction for cancer detection and therapy.

5. Conclusions

In this work, voltage-gated ion channels were modeled as control objects or systems by applying the control system theory and a system identification method. The Kv10.1 voltage-gated ion channel exhibits dynamic behavior as a first-order dynamic system. We presented a classical control algorithm and described how this algorithm could theoretically be used to control the response of the Kv10.1 voltage-gated ion channel. Other control algorithms, such as robust control or fuzzy control, could also be used. Research has shown that controlling the Kv10.1 ion channel under up-regulated conditions plays a vital role in cancer prevention and treatment. Nanoelectromechanical systems, such as nanorobots, could be used in the treatment of cancer as they are able to travel through the blood vessel system to the target cells and bind to the ion channels. The robot's control unit can then be activated based on the implemented control algorithm, and the desired ion channel regulation can be performed to treat channel activity by the down or upregulation of the targeted channels.

It is, therefore, expected that such models, which could also describe the activity of multiple ion channels and their interactions, e.g., described by a MIMO system, will enable the use of nanoelectromechanical systems and nanorobots, as demonstrated for the Kv10.1 voltage-gated ion channel, and for other ion channel families, with the goal of establishing new tools for cancer detection and treatment at the single-cell level.

Author Contributions: Conceptualization, J.L.Š.; methodology, J.L.Š.; validation, J.L.Š.; formal analysis, J.L.Š.; investigation, J.L.Š. and S.L.; resources, C.B.; data curation, J.L.Š. and S.L.; writing—original draft preparation, J.L.Š.; writing—review and editing, J.L.Š., S.L. and C.B.; visualization, J.L.Š.; supervision, J.L.Š. and C.B. All authors have read and agreed to the published version of the manuscript.

Funding: Open Access Funding by the Graz University of Technology.

Institutional Review Board Statement: Not applicable.

Informed Consent Statement: Not applicable.

Data Availability Statement: https://channelpedia.epfl.ch/ionchannels/ (accessed on 15 February 2022).

Acknowledgments: We acknowledge Open Access Funding by Graz University of Technology.

Conflicts of Interest: The authors declare no conflict of interest.

References

1. Tan, A.; Jeyaraj, R.; De Lacey, S.F. Nanotechnology in Neurosurgical Oncology. In *Nanotechnology in Cancer*; Elsevier: Amsterdam, The Netherlands, 2017; pp. 139–170. ISBN 978-0-323-39080-4.
2. Requicha, A.A.G. Nanorobots, NEMS, and Nanoassembly. *Proc. IEEE* **2003**, *9*, 1922–1933. [CrossRef]
3. Simovic-Pavlovic, M.; Bokic, B.; Vasiljevic, D.; Kolaric, B. Bioinspired NEMS—Prospective of Collaboration with Nature. *Appl. Sci.* **2022**, *12*, 905. [CrossRef]
4. Giri, G.; Maddahi, Y.; Zareinia, K. A Brief Review on Challenges in Design and Development of Nanorobots for Medical Applications. *Appl. Sci.* **2021**, *11*, 10385. [CrossRef]
5. Asher, V.; Sowter, H.; Shaw, R.; Bali, A.; Khan, R. Eag and HERG Potassium Channels as Novel Therapeutic Targets in Cancer. *World J. Surg. Oncol.* **2010**, *8*, 113. [CrossRef]
6. García-Becerra, R.; Díaz, L.; Camacho, J.; Barrera, D.; Ordaz-Rosado, D.; Morales, A.; Ortiz, C.S.; Avila, E.; Bargallo, E.; Arrecillas, M.; et al. Calcitriol Inhibits Ether-à Go-Go Potassium Channel Expression and Cell Proliferation in Human Breast Cancer Cells. *Exp. Cell Res.* **2010**, *316*, 433–442. [CrossRef]
7. Wang, G.J.; Chen, C.L.; Hsu, S.H.; Chiang, Y.L. Bio-MEMS Fabricated Artificial Capillaries for Tissue Engineering. *Microsyst. Technol.* **2005**, *12*, 120–127. [CrossRef]
8. Tsuda, S.; Zauner, K.-P.; Gunji, Y.-P. Robot Control with Biological Cells. *Biosystems* **2007**, *87*, 215–223. [CrossRef]
9. Mendonça Munhoz, A.; Santanelli di Pompeo, F.; De Mezerville, R. Nanotechnology, Nanosurfaces and Silicone Gel Breast Implants: Current Aspects. *Case Rep. Plast. Surg. Hand Surg.* **2017**, *4*, 99–113. [CrossRef]
10. Ion Channel | Learn Science at Scitable. Available online: https://www.nature.com/scitable/topicpage/ion-channel-14047658/ (accessed on 7 April 2022).
11. Marchesi, A.; Gao, X.; Adaixo, R.; Rheinberger, J.; Stahlberg, H.; Nimigean, C.; Scheuring, S. An Iris Diaphragm Mechanism to Gate a Cyclic Nucleotide-Gated Ion Channel. *Nat. Commun.* **2018**, *9*, 3978. [CrossRef]
12. Shad, K.F.; Salman, S.; Afridi, S.; Tariq, M.; Asghar, S. Introductory Chapter: Ion Channels. In *Ion Channels in Health and Sickness*; Shad, K.F., Ed.; InTech: London, UK, 2018; ISBN 978-1-78984-227-2.
13. Gabashvili, I.S.; Sokolowski, B.H.A.; Morton, C.C.; Giersch, A.B.S. Ion Channel Gene Expression in the Inner Ear. *J. Assoc. Res. Otolaryngol.* **2007**, *8*, 305–328. [CrossRef]
14. Sands, Z.; Grottesi, A.; Sansom, M.S.P. Voltage-Gated Ion Channels. *Curr. Biol.* **2005**, *15*, R44–R47. [CrossRef] [PubMed]
15. EPFL Blue Brain Project, Channelpedia. Available online: https://channelpedia.epfl.ch/ (accessed on 7 April 2022).
16. Coetzee, W.A.; Amarillo, Y.; Chiu, J.; Chow, A.; Lau, D.; McCormack, T.; Morena, H.; Nadal, M.S.; Ozaita, A.; Pountney, D.; et al. Molecular Diversity of K+ Channels. *Ann. N. Y. Acad. Sci.* **1999**, *868*, 233–255. [CrossRef] [PubMed]
17. Jan, L.Y.; Jan, Y.N. Voltage-Gated and Inwardly Rectifying Potassium Channels. *J. Physiol.* **1997**, *505*, 267–282. [CrossRef] [PubMed]
18. Serrano-Novillo, C.; Capera, J.; Colomer-Molera, M.; Condom, E.; Ferreres, J.; Felipe, A. Implication of Voltage-Gated Potassium Channels in Neoplastic Cell Proliferation. *Cancers* **2019**, *11*, 287. [CrossRef] [PubMed]
19. Lastraioli, E.; Iorio, J.; Arcangeli, A. Ion Channel Expression as Promising Cancer Biomarker. *Biochim. Biophys. Acta BBA-Biomembr.* **2015**, *1848*, 2685–2702. [CrossRef]
20. Asher, V.; Khan, R.; Warren, A.; Shaw, R.; Schalkwyk, G.V.; Bali, A.; Sowter, H.M. The Eag Potassium Channel as a New Prognostic Marker in Ovarian Cancer. *Diagn. Pathol.* **2010**, *5*, 78. [CrossRef]
21. Langthaler, S.; Lozanović Šajić, J.; Rienmüller, T.; Weinberg, S.H.; Baumgartner, C. Ion Channel Modeling beyond State of the Art: A Comparison with a System Theory-Based Model of the Shaker-Related Voltage-Gated Potassium Channel Kv1.1. *Cells* **2022**, *11*, 239. [CrossRef]
22. Ogata, K. *Modern Control Engineering*, 5th ed.; Prentice-Hall Electrical Engineering Series. Instrumentation and Controls Series; Prentice-Hall: Boston, MA, USA, 2010; ISBN 978-0-13-615673-4.
23. Schoukens, J.; Pintelon, R.; Rolain, Y. *Mastering System Identification in 100 Exercises*; Wiley: Hoboken, NJ, USA, 2012; ISBN 978-0-470-93698-6.
24. Dorf, R.C.; Bishop, R.H. *Modern Control Systems*, 13th ed.; Pearson: Hoboken, NJ, USA, 2016; ISBN 978-0-13-440762-3.
25. Nise, N.S. *Control Systems Engineering*, 7th ed.; Wiley: Hoboken, NJ, USA, 2015; ISBN 978-1-118-17051-9.
26. Ljung, L. *System Identification: Theory for the User*, 2nd ed.; Prentice Hall Information and System Sciences Series; Prentice Hall PTR: Upper Saddle River, NJ, USA, 1999; ISBN 978-0-13-656695-3.
27. Ljung, L. *System Identification Toolbox™ User's Guide*; The MathWorks, Inc.: Natick, MA, USA, 2014.

28. Option Set for Tfest-MATLAB-MathWorks Switzerland. Available online: https://ch.mathworks.com/help/ident/ref/tfestoptions.html (accessed on 7 April 2022).
29. Delgado-Ramírez, M.; De Jesús-Pérez, J.J.; Aréchiga-Figueroa, I.A.; Arreola, J.; Adney, S.K.; Villalba-Galea, C.A.; Logothetis, D.E.; Rodríguez-Menchaca, A.A. Regulation of Kv2.1 Channel Inactivation by Phosphatidylinositol 4,5-Bisphosphate. *Sci. Rep.* **2018**, *8*, 1769. [CrossRef]
30. Martínez, R.; Stühmer, W.; Martin, S.; Schell, J.; Reichmann, A.; Rohde, V.; Pardo, L. Analysis of the Expression of Kv10.1 Potassium Channel in Patients with Brain Metastases and Glioblastoma Multiforme: Impact on Survival. *BMC Cancer* **2015**, *15*, 839. [CrossRef]
31. Lazic, D. *Nelinearni Sistemi (Nonlinear Systems)*; Faculty of Mechanical Engineering, University of Belgrade: Belgrade, Serbia, 2005; ISBN 978-86-7083-530-6.
32. Wang, W.; Wu, Z.; He, Q. Swimming Nanorobots for Opening a Cell Membrane Mechanically. *View* **2020**, *1*, 20200005. [CrossRef]
33. Ouadid-Ahidouch, H.; Ahidouch, A.; Pardo, L.A. Kv10.1 K+ Channel: From Physiology to Cancer. *Pflüg. Arch.-Eur. J. Physiol.* **2016**, *468*, 751–762. [CrossRef] [PubMed]
34. Yang, R.; Xi, N.; Lai, K.W.C.; Patterson, K.C.; Chen, H.; Song, B.; Qu, C.; Zhong, B.; Wang, D.H. Cellular Biophysical Dynamics and Ion Channel Activities Detected by AFM-Based Nanorobotic Manipulator in Insulinoma β-Cells. *Nanomed. Nanotechnol. Biol. Med.* **2013**, *9*, 636–645. [CrossRef] [PubMed]
35. Pardo, L.A. Oncogenic Potential of EAG K+ Channels. *EMBO J.* **1999**, *18*, 5540–5547. [CrossRef] [PubMed]
36. Cázares-Ordoñez, V.; Pardo, L.A. Kv10.1 Potassium Channel: From the Brain to the Tumors. *Biochem. Cell Biol.* **2017**, *95*, 531–536. [CrossRef]
37. Li, S.; Jiang, Q.; Ding, B.; Nie, G. Anticancer Activities of Tumor-Killing Nanorobots. *Trends Biotechnol.* **2019**, *37*, 573–577. [CrossRef]
38. Hariharan, R.; Manohar, J. Nanorobotics as Medicament: (Perfect Solution for Cancer). In Proceedings of the INTERACT-2010, Chennai, India, 3–5 December 2010; IEEE: Chennai, India, 2010; pp. 4–7.
39. Manjunath, A.; Kishore, V. The Promising Future in Medicine: Nanorobots. *Biomed. Sci. Eng.* **2014**, *2*, 42–47. [CrossRef]